Werk

Jahr: 1981
Kollektion: fid.geo
Signatur: 8 Z NAT 2148:50
Digitalisiert: Niedersächsische Staats- und Universitätsbibliothek Göttingen
Werk Id: PPN1015067948_0050
PURL: http://resolver.sub.uni-goettingen.de/purl?PPN1015067948_0050

LOG Id: LOG_0046
LOG Titel: Energy dispersion and acceleration of low energy protons and their relation to electrons during an auroral breakup
LOG Typ: article

Übergeordnetes Werk

Werk Id: PPN1015067948
PURL: http://resolver.sub.uni-goettingen.de/purl?PPN1015067948
OPAC: http://opac.sub.uni-goettingen.de/DB=1/PPN?PPN=1015067948

Contact

Niedersächsische Staats- und Universitätsbibliothek Göttingen
Georg-August-Universität Göttingen
Platz der Göttinger Sieben 1
37073 Göttingen
Germany
Email: gdz@sub.uni-goettingen.de

J Geophys (1982) 50:189–193

Journal of Geophysics

Energy Dispersion and Acceleration of Low Energy Protons and Their Relation to Electrons During an Auroral Breakup

A. Urban[1], K.M. Torkar[1], and K. Wilhelm[2]

[1] Space Research Institute of the Austrian Academy of Sciences, c/o Technical University Graz, A-8010 Graz, Inffeldgasse 12, Austria
[2] Max-Planck-Institut für Aeronomie, D-3411 Katlenburg-Lindau 3, Federal Republic of Germany

Abstract. This paper describes a "proton time-of-flight event" observed onboard a high altitude rocket in the auroral zone during a magnetospheric substorm expansion phase. The onset was defined by a rapid low energy electron influx enhancement. After 36–55 s three successive peaks at 13, 7 and 5.5 keV were measured by the low energy proton detectors and related to the increase of the intense electron precipitation. On the assumption that the spectral variations of the protons were caused by energy dispersion, a distance to the proton acceleration or precipitation region of $\sim 9\ R_E$ was evaluated. Generally, the measured differential proton spectra for the flight could be fitted by a power law $F = F_0\ E^{-\gamma}$ with a slope of $\gamma \sim 0.7$, except for the event mentioned above and two other events discussed in relation to the simultaneously measured electron precipitation. The pitch angle distribution of the protons was typically isotropic over the upper hemisphere.

Key words: Particle acceleration – Energy dispersion – Mono-energetic protons – Substorm expansion phase

Introduction

The fluxes of low energy protons and electrons in the keV-range show all sorts of different relations, and all combinations of flux and spectral variations can be found in limited regions. The most commonly occurring combinations in this energy range seem to be the correlation in flux variations and anti-correlations in the spectral hardness variation. When the precipitating proton flux increases, its spectrum softens, simultaneously the electron flux also increases and the electron spectrum hardens (Johnstone 1971; Bryant et al. 1977; Edwards et al. 1978; Urban 1981). However, Miller and Whalen (1976) reported the lack of any consistent correlation between electron and proton precipitation. Whalen et al. (1978) came to a similar conclusion stating that no definite relations between proton and electron fluxes exist.

Proton energy spectra with peaks in the keV range were observed by Whalen et al. (1971), Whalen and McDiarmid (1972) and by Miller and Whalen (1976). They attributed the spectral peaks to electrostatic potential drops, but found no clear relation to the electron measurements. Bryant et al. (1977) reported a similar behaviour where a spectral peak developed at ~ 6 keV together with a small proton flux increase without any obvious change in the electron population.

The pitch angle distributions of low energy protons in the keV-range have been found to be rather isotropic or, in some cases, to peak at 90° (Johnstone 1971; Miller and Whalen 1976). Field aligned proton pitch angle distributions have been observed mainly by means of low-orbiting satellites (Hultqvist 1971; Hultqvist and Borg 1978), but also with rockets (Urban 1981; Brüning et al. 1981). The observed pitch angle distributions peaking at a few tens of degrees above 90° ("conical beams", Whalen et al. 1978) are not discussed in this paper. Here the data from simultaneous rocket-borne proton and electron measurements in the keV-range observed during an auroral breakup are presented. They show a clear correlation in the proton and electron flux variations.

In particular, the measured proton spectral variations with a sequence of peaks in the energy range 13–5 keV are related to the intense electron precipitation mentioned above and interpreted in terms of energy dispersion of the protons over a distance of about 9 Earth radii.

Instrumentation

The payload F4C was launched on 30 January 1978 at 21:37 UT by a Skylark-12 motor from the Andøya Rocket Range, Norway, and reached an apogee of 530 km. The actual launch azimuth was 346°. The payload had an attitude control system so that the spin axis had an angular deviation of $20° \pm 10°$ with respect to the negative geomagnetic field direction. The spin period was approximately 350 ms.

The complex experimental equipment of the payload allowed particle and field observations in wide energy and frequency ranges. F4C was one of four high altitude sounding rocket payloads of the German IMS campaign "Substorm Phenomena" launched from the Andøya Rocket Range during the time period 13 October 1977–30 January 1978 (Wilhelm 1980).

The proton measurements in the energy range 0.5–30 keV were obtained by 80° spherical electrostatic analysers as energy selectors and channel electron multipliers operating in pulse counting modes as particle detectors. After the energy selection the protons were post-accelerated by a negative potential of 1.3 kV in order to compensate the lower efficiency of the channel electron multiplier for protons at low energies.

The energy spectra in the range 0.5–30 keV were scanned in 19 logarithmic levels with 20 ms sampling time each. A summary of the relevant parameters of the instrument is compiled in Table 1. Three of these proton detectors were mounted at 0°, 20° and 90° with respect to the spin axis. Each sensor was calibrated in order to determine the entrance characteristic, the geometric factor, and the efficiency and energy dependence of the channel electron multipliers. For technical reasons this calibration procedure was performed using a mono-energetic elec-

0340-062X/82/0050/0189/$01.00

Table 1. Characteristics of the instruments

		Proton-Spectr.	Electron-Spectr.
Energy range	keV	0.5–30	0.05–25
Resolution $\Delta E/E$	%	7.5	7
Geometric factor	cm^2 sr	4×10^{-3}	2×10^{-3}
Field of view	deg^2	8×10	$24 \times 4 \times 6$
Time for one spectrum	s	0.4	46 or 1.5

tron beam with varying acceleration potentials of the beam and horizontal and vertical viewing angles of the sensor. The different efficiencies of the channeltrons for protons compared to electrons were accounted for by use of conversion methods published in the literature (Egidi et al. 1969; Iglesias and McGarity 1971; Crandall and Ray 1975).

The electrons were measured by a differential energy and angle analyser with a field of view of $96° \times 6°$ subdivided into 24 angular sections. The energy selection was performed by two 80° spherical electrostatic analysers. Auxiliary electrostatic deflection devices selected the 24 angular channels. This scheme enabled the experiment to measure directional electron fluxes with a coverage of about 96° in pitch angle range without even utilizing the rocket spin. The instrument operated in slow and fast measurement modes. During the slow mode the viewing direction was controlled by the onboard magnetometer and the selection energy changed slowly in approximately 46 s over the full energy range. During the fast mode the selection energy swept quickly within 1.5 s.

Geophysical Conditions

The payload F4C was launched at 21:37 UT during the expansive phase of a magnetospheric substorm. The K_p value during the time interval from 21–24 UT was -5. The disturbance to be discussed here was preceded by a 100 nT depression of the X-component of the geomagnetic field (Fig. 1). The activity of the northernmost of the two stable auroral arcs located above Andøya intensified, and later on, at 21:30 UT, a violent breakup occurred, followed by an increase in brightness of the southern arc. Four minutes later the whole sky was covered by auroral displays. The brightness values measured at 21:32 UT, although somewhat uncertain because of a high altitude cloud layer, were 100 kR for $\lambda = 557.7$ nm, 3.6 kR for 630.0 nm, and 200 R for 486.1 nm. Unfortunately, an additional low altitude cloud cover caused a rapid deterioration of the visibility immediately after the launch of F4C preventing all sky and photometer observations. Recordings of the geomagnetic variations and pulsations during this event are shown in Figures 1 and 2. The X-component decreased by approximately 500 nT within several minutes concurrently with the fast expansion of the aurora. The large variations of the Y-component were associated with auroral forms directed south-east to north-west.

The geomagnetic pulsations (Fig. 2) showed large amplitudes in both H and D components between 21:30 UT. During the flight of F4C the amplitudes decreased from 30 to about 20 nT. Thereafter the substorm recovered rapidly, interrupted only by some activity increase after 22:30 UT.

Observations

A summary of the low energy proton and electron measurements is given in Figure 3. The different time resolutions apparent

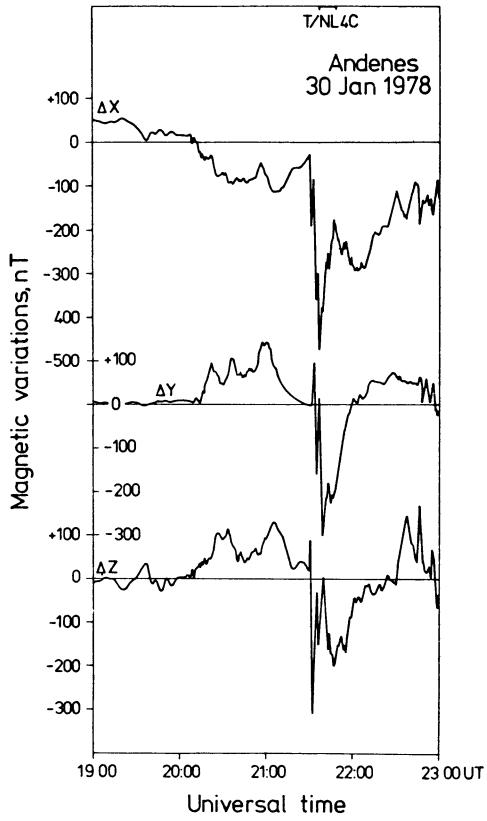

Fig. 1. Variations of the geomagnetic field at Andøya on 30 January 1978. The flight time of the rocket payload T/NL-F4C is indicated at the top of this figure. The variations of the north, east and vertical components are denoted ΔX, ΔY and ΔZ, respectively

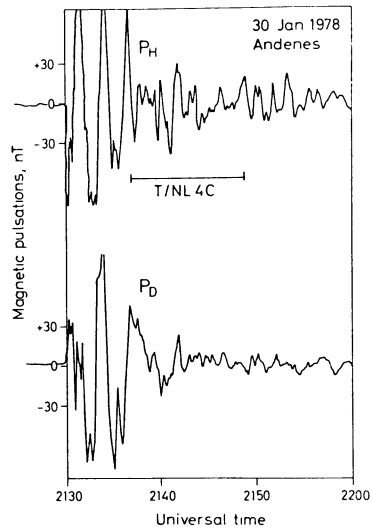

Fig. 2. Horizontal components of the magnetic pulsation activity at Andøya during the flight period of F4C

in the electron fluxes result from the different operating modes of the instrument. Hence the solid line between 160 and 285 s represents three differential energy spectra with high pitch angle resolution, whereas before that time differential energy spectra with high energy resolution have been measured.

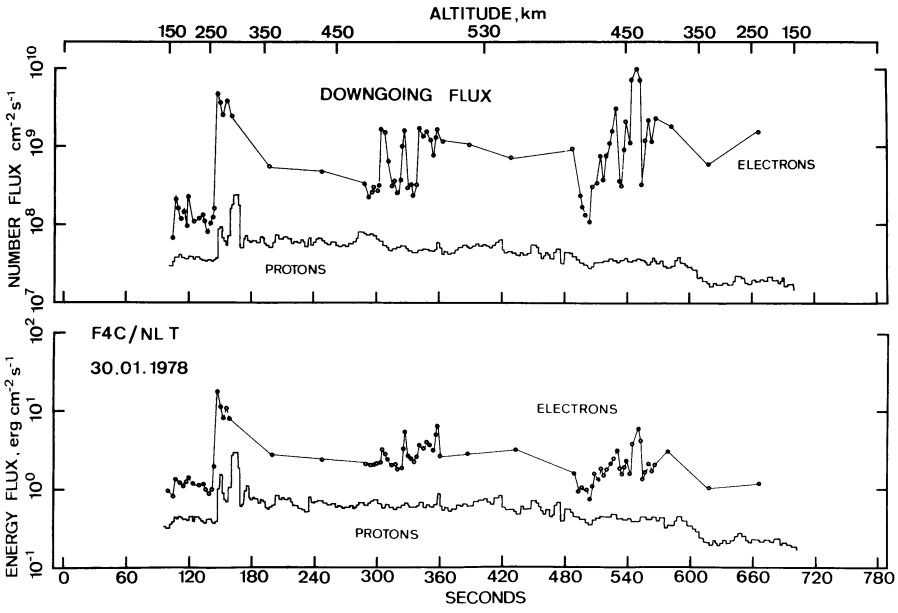

Fig. 3. Downward directed proton and electron energy fluxes and number fluxes during the flight F4C. The variable time resolution apparent in the electron fluxes results from different operating modes of the instrument. The observed proton spectral variations are related to the sudden flux increase at 151 s

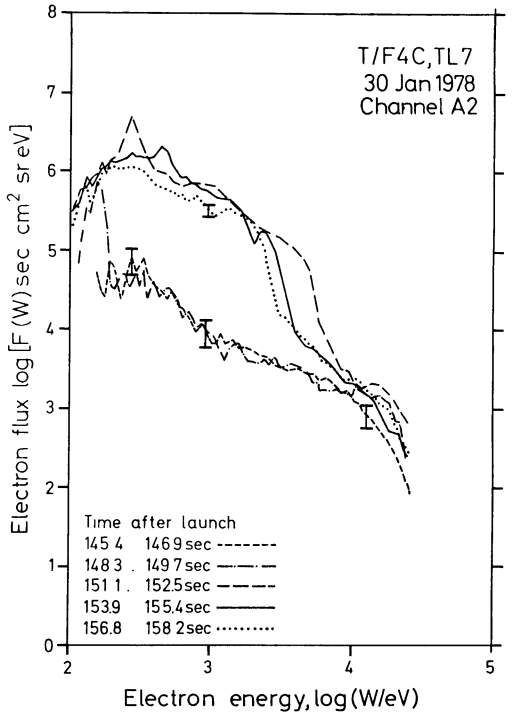

Fig. 4. Electron energy spectra before and after the flux increase at 151 s during flight F4C. Note the dramatic rise of the intensity of electrons below 5 keV only

At 151 s the downgoing proton energy and number fluxes in the energy range 0.5 to 30 keV increase simultaneously with the electron fluxes. Twenty seconds later a stronger precipitation of protons occured for some seconds. During the rest of the flight the proton energy influx remained at a nearly constant level of 0.7 erg $cm^{-2}\,s^{-1}$ at a height of 350 km, where charge exchange reactions become more and more important.

The above two time periods, and that after 500 s when the electron spectrometer is in the right mode to observe fast variations, are selected for comparisons with the proton data.

The electron energy spectra for the time interval near the first flux increase at 151 s have been compiled in Figure 4. The spectra just before the increase were relatively flat in the energy range 0.1 keV to approximately 10 keV The high energy flux after 151 s was carried by electrons with energies between 0.1–5 keV. During the flux enhancement of nearly two orders of magnitude the high energy cutoff decreased from 5 to 2.4 keV within 6–7 s.

In the upper part of Figure 5 the energy channel 0.75 keV is plotted on an expanded time scale between 100 s and 220 s. At the onset of the intense electron precipitation (at 151 s flight time) a sudden increase of the intensity of the proton fluxes of 0.75 keV appeared. After 3 s the intensity decreased again and at 166 s the proton flux reached a new peak value one order of magnitude higher than the average flux. After 170 s the differential proton flux had an average value of 2×10^6 protons $cm^{-2}\,sr^{-1}\,s^{-1}\,keV^{-1}$ Three differential proton energy spectra from this event are shown in the bottom part of Figure 5. At 167 s, the intensity was approximately one order of magnitude higher in the full measured energy range 0.5–30 keV. The dashed line indicates the proton energy spectrum at 155 s in order to facilitate the comparison.

Interesting observations related to the enhanced electron precipitation near 151 s were not obtained only as spectral variations of the electrons, as illustrated in Figure 4, but also as a variation of the proton energy distribution (Fig. 6). Three successive peaks in the proton spectra were measured, the first at a peak energy of 13 keV, followed 13 s later by one at 7 keV and 6 s later by a 5.5 keV peak. These three peaks were the most remarkable and appeared for some seconds, whereas the dispersion of other energies could not be clearly identified due to some flux intensity variations during that time. A fourth peak at 9.3 keV fitting into the sequence was measured between 192 and 196 s, but has been omitted as it failed to reach statistical significance and fell within an energy range only coarsely covered by the instruments. These observations led us to assume that the change in the proton spectra was caused by energy dispersion. This will be discussed in the next section. The pitch angle distribution of the protons during these successive peaks was isotropic inside the loss cone.

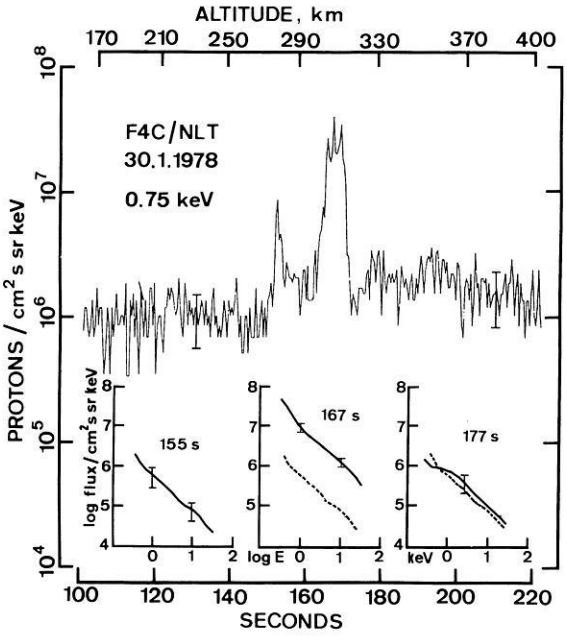

Fig. 5. The 0.75 keV proton channel during the intense electron precipitation in an expanded time scale. In the lower part three differential energy spectra of the protons are compiled demonstrating the intensity increasing in the full energy range

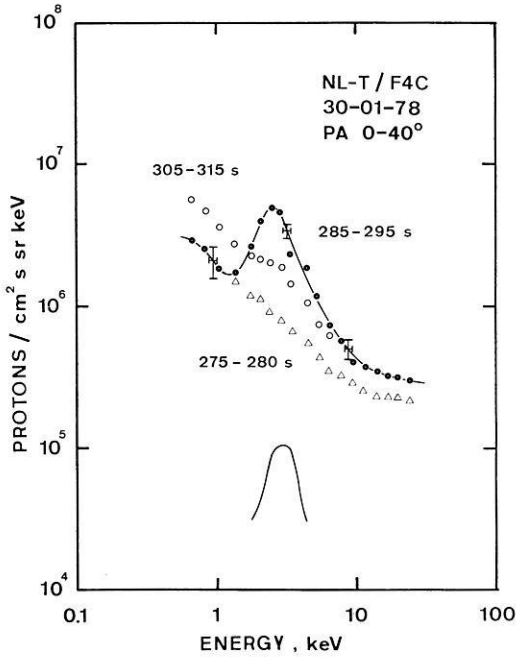

Fig. 7. Proton energy spectrum with the appearance of a mono-energetic peak before the large variations of the electron number flux at 300 s. Below the detector response to mono-energetic particles, as obtained from the calibration procedure of the sensor, is indicated

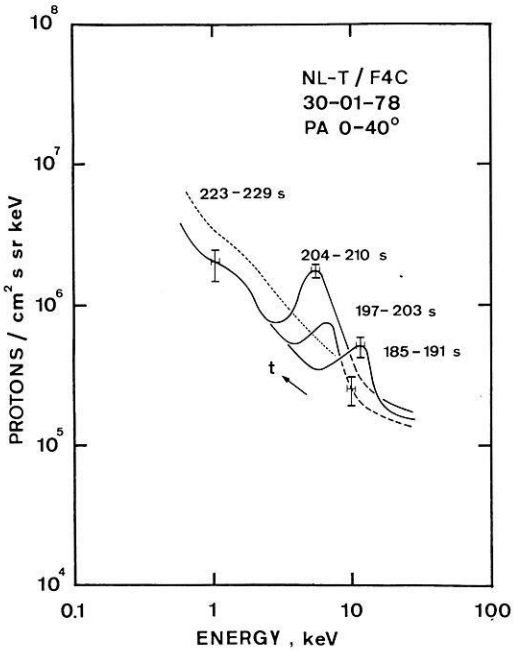

Fig. 6. Proton spectral variations showing energy dispersion effects in relation to the increase of electrons at 151 s. From the time of the appearance of the most marked energy peaks, the distance of the proton precipitation region was evaluated

Further peaked proton spectra were measured during this flight at 290 s and 485 s after launch. The differential energy spectrum in the time interval 285 to 295 s is plotted in Figure 7 and shows a remarkable peak at 3 keV. Below, the response of the detector to monoenergetic electrons, obtained from the calibration, is indicated. The peak rose from a power law spectrum $F(E)=F_0\,E^{-\gamma}$ typical for this flight with a spectral coefficient of $\gamma\sim 0.7$. The flux remained very constant during approximately 20 s and then dropped to a power law spectrum which is a factor 2 or 3 higher than prior to the peak formation. At the same time a large variation in the electron number flux was detected (see Fig. 3). The pitch angle distribution at the proton peak energy 2.9 keV was a typical loss cone distribution during this event.

The other isolated peak in the proton energy spectra was observed within the time interval 483–487 s after launch. The pitch angle distribution at the peak energy 5.36 keV was isotropic before, during, and after the peak.

Discussion and Conclusion

What are the conclusions that can be drawn from the reported observations with respect to the rapid electron energy flux enhancement at 151 s? Under the assumption that the electron enhancement defines the onset time (t_0) for an energy dispersion of the observed variations of the proton spectra (Fig. 6), we calculated the distance s of the proton precipitation region from the proton energy, E_p, and mass, m_p, using the basic formula (1) and

$$s=v_p\cdot t=\sqrt{\frac{2\,E_p}{m_p}}\cdot t \qquad (1)$$

the transit time t of the protons with the well developed peak energy (Table 2).

For the source distance s statistical uncertainties are calculated from the time where the flux intensity reached 70% of the maximum at the corresponding peak energy. The start time of the velocity dispersion event has been set at 150 s.

For all protons with peak energies we obtained a distance from the source region of approx. 9 Earth radii (R_E). Along a geomagnetic fieldline (dipole model) which is crossed by a rocket at an L-value of approx. 7 the distance from the Earth to the equatorial region is approx. 9 R_E.

Table 2. Compiled parameters transit time t at the maximum flux intensity E_p, velocity v_p and distance s evaluated from the energy dispersion, t_0 = onset time

t after $t_0 = 150$ s	E_p [keV]	v_p [m/s]	s [m]
$t_0 + 37$ s	13	1.58×10^6	$(58.6 \pm 2.5) \times 10^6$
$t_0 + 50$ s	7	1.16×10^6	$(58.1 \pm 2.4) \times 10^6$
$t_0 + 56$ s	5.5	1.03×10^6	$(58.7 \pm 2.1) \times 10^6$

At $t = 150$ s after launch an as yet unexplained diffusion mechanism precipitated electrons and protons in the equatorial region into the local loss cone. The transit time of the electrons (of the order of one second) was very short compared to the transit time of the protons (37 to 56 s) and their arrival (at 151 s) indicates the start of the event as being approx. one second before.

The dispersion calculation is based on the assumption that the ions are protons and not heavier ions (e.g. O^+). No velocity changes due to acceleration or deceleration in field aligned electric fields are included in the model because the field mentioned below disappeared before the protons of the primary source could be affected.

In addition to the sudden increase of the precipitation of the low energy electrons (with an energy < 5 keV) Wilhelm and Stüdemann (in press 1982) reported an energy shift in the electron spectrum together with a post-acceleration of energetic electrons by a 5 kV potential difference. As a mechanism for generating a potential drop, Hultqvist (1971) proposed an interaction between the hot magnetospheric plasma and the cold ionospheric plasma during intense electron precipitation.

No sufficient explanation can be given for the high intensities of the proton fluxes at around 167 s with a duration of some seconds. The electron data were measured in a slow sweep mode, so that the interpretation is rather difficult.

The large variations of the electron number flux at about 300 s were accompanied for 20 s by a well developed peak of the proton spectra at 3 keV. Bryant et al. (1977) reported a similar observation when the rocket crossed from a stable auroral arc into a diffuse aurora. Unfortunately, all-sky photographs or photometer recordings do not exist from flight F4C because of the overcast sky, so that no direct comparison can be made.

A further isolated peak of the proton energy spectra at 5.36 keV with a differential flux ratio of three above the background was observed later from 483–487 s. The assumption of a proton acceleration by a potential drop directed to the Earth and located at higher altitudes is supported by the strong decay of electrons at lower energies at that time. Comparing the strong decrease of the electron number flux at about 500 s to the continued, fairly constant electron energy flux in Figure 3 one may recognize a loss of electrons with lower energies, possibly retarded by a potential drop.

Any related proton energy flux increase one might expect is not observed. However, around that time there is a decreasing slope for both electrons and protons possibly due to a weakening of a common precipitation mechanism, which could counteract the effects of the potential drop.

Acknowledgements. The project "Substorm Phenomena" was supported financially by the German Bundesministerium für Forschung und Technologie. The Austrian contribution was made possible by grants of the Austrian Academy of Sciences and the Austrian Council for Scientific Research.

References

Brüning, K., Baumjohann, W., Wilhelm, K., Stüdemann, W., Urban, A., Ott, W., Spenner, K., Schmidtke, G.L., Fischer, H.M.: Application of different methods for the determination of ionospheric conductivities from sounding rocket observations. J. Geophys. **49**, 74–81, 1981

Bryant, D.A., Hall, D.S., Lepine, D.R., Mason, R.W.N.: Electrons and positive ions in an auroral arc. Nature **266**, 148–149, 1977

Crandall, D.H., Ray, J.A.: Channeltron efficiency for counting of H^+ and H^- at low energy. Rev. Sci. Instr. **46**, 562–564, 1975

Edwards, T., Bryant, D.A., Smith, M.J.: Preliminary results of particle measurements from Skylark SL 1421 and Fulmar F1. Paper presented ad MIST, Southampton, 7 April, 1978

Egidi, A., Marconero, R., Pizella, G., Sperli, F.: Channeltron fatigue and efficiency for protons and electrons. Rev. Sci. Instr. **40**, 88–91, 1969

Hultqvist, B.: On the productions of magnetic field aligned electric fields by the interaction between the hot magnetospheric plasma and the cold ionosphere. Planet. Space Sci. **19**, 149–158, 1971

Hultqvist, B., Borg, H.: Observations of energetic ions in inverted V-events. Planet. Space Sci. **26**, 673–689, 1978

Iglesias, G.E., McGarity, J.O.: Channel electron multiplier efficiency for protons of 0.2 to 10 keV Rev. Sci. Instr. **42**, 1728–1729, 1971

Johnstone, A.D.: Correlation between electron and proton fluxes in post-breakup aurora. J. Geophys. Res. **76**, 5259–5267, 1971

Miller, J.R., Whalen, B.A.: Characteristics of auroral proton precipitation observed from sounding rockets. J. Geophys. Res. **81**, 147–154, 1976

Urban, A.: Measurements of low energy auroral ions. Planet. Space Sci. **29**, 1353–1365, 1981

Whalen, B.A., Miller, J.R., McDiarmid, I.B.: Evidence for a solar wind origin of auroral ions from low-energy ion measurements. J. Geophys. Res. **76**, 2406–2418, 1971

Whalen, B.A., McDiarmid, I.B.: Further low-energy auroral ion composition measurements. J. Geophys. Res. **77**, 1306–1310, 1972

Whalen, B.A., Bernstein, W., Daly, P.W.: Low altitude acceleration of ionospheric ions. Geophys. Res. Lett. **5**, 55–58, 1978

Wilhelm, K.: Study of magnetospheric substorm events. ESA-SP **152**, 269–277, 1980

Wilhelm, K., Stüdemann, W.: Evidence of field-aligned electrostatic acceleration of auroral electrons. J. Geophys., in press 1982

Received May 25, 1981; Revised version November 16, 1981
and January 22, 1982
Accepted January 28, 1982